THE ASTROPHYSICAL JOURNAL, 316:189–205, 1987 May 1

DEEP CCD PHOTOMETRY IN GLOBULAR CLUSTERS. V. M5

HARVEY B. RICHER[1] AND GREGORY G. FAHLMAN[1]
Department of Geophysics and Astronomy, University of British Columbia
Received 1986 July 10; accepted 1986 October 15

ABSTRACT

Deep *UBV* CCD imagery has been obtained in three fields of the galactic globular cluster M5. The locations of these fields are at distances of 8, 21, and 58 core radii. In the middle field, which overlaps substantially with the deep photometry field of Arp, the CCD photometry reaches fainter than $V = 26$. Color-magnitude diagrams constructed from stars in the inner two fields are identical, to within the errors, and can be used to set an upper limit of 4% to any metallicity difference between these two fields. A U, $(U-V)$ color-magnitude diagram is also shown for the inner field and compared with that of a more metal rich and more metal poor cluster. Major differences in the morphology of these three diagrams are present as a function of metal abundance. From the color-color diagram of the cluster, together with published values, the reddening in the direction of M5 is estimated to be $E(B-V) = 0.02$ and its metallicity is determined to be $[M/H] = -1.13$. The distance to M5 is then established from fitting local subdwarfs to the lower main sequence of the cluster. This yields $(m-M)_v = 14.30$. Using the observationally determined parameters an overlay of the appropriate VandenBerg and Bell isochrones yields an age estimate of 17 Gyr for M5. Luminosity functions constructed from the three fields show excellent agreement through the range $V = 17$ to 23. Fainter than $V = 23$ there is some evidence for mass segregation effects due to dynamical relaxation.

Subject headings: clusters: globular — photometry — stars: evolution

I. INTRODUCTION. OBSERVATIONS AND DATA REDUCTION

This paper, the fifth in our series on CCD photometry of galactic globular clusters, is devoted to M5. Previous contributions have dealt with M4 (Richer and Fahlman 1984; Fahlman and Richer 1987), M15 (Fahlman, Richer, and VandenBerg 1985) and M13 (Richer and Fahlman 1986). Our work and that of others on galactic globulars using linear, digital detectors (e.g., 47 Tuc [Harris and Hesser 1985], Pal 4 [Christian and Heasley 1986], NGC 6752 [Penny and Dickens 1986], M13 [Lupton and Gunn 1986]) have resulted in the following conclusions. (1) The cluster main-sequences have virtually zero intrinsic width. This is of importance since it can set tight constraints on any metal or He abundance variation among the cluster stars as well as provide an estimate of the dispersion in rotational velocity among member stars. Limits of less than 30% star-to-star metal abundance variation have already been established for M4 (Richer and Fahlman 1984) and M13 (Richer and Fahlman 1986). (2) Except possibly for the globular cluster E3 (McClure *et al.* 1985), no system yet investigated with panoramic digital detectors exhibits any evidence for a binary sequence among its main-sequence stars. For M4 and M13 we were able to show that the percentage of nearly equal mass binaries among the main-sequence stars did not exceed a few percent. (3) In a recent paper, McClure *et al.* (1986) showed that if the mass functions of the galactic globulars can be described by a power law, then there was a remarkable relation between the exponent of the power law and the metal abundance of the cluster. This correlation was in the sense that the more metal poor the cluster, the steeper the power law. The most reasonable interpretation of this result is that it reflects the initial mass function (IMF) of the system, and, while it is difficult to imagine that it is due to dynamical evolution, we investigate this in this paper by examining the luminosity function in three radial fields of M5. (4) The ages of those globular clusters studied recently with digital detectors whose photometry is accurate to at least 2 mag below the turnoff all seem to be in the range of 16–18 Gyr. No convincing evidence has yet been found for any real age difference among the galactic globulars, and this includes the two distant Palomar clusters Pal 4 (Christian and Heasley 1986) and Pal 5 (Smith *et al.* 1986).

M5, being relatively nearby and populous, has been the subject of several photometric studies in the past. Arp (1955, 1962) produced a remarkable photographic color-magnitude diagram (CMD) extending three magnitudes below the turnoff, while the brighter cluster stars have been investigated by Simoda and Tanikawa (1970) and Buonanno, Corsi, and Fusi Pecci (1981). Our aim in this investigation is to go significantly deeper than these studies, produce data that are carefully calibrated, look for radial effects in both the CMD of the cluster and its luminosity function since such effects may indicate abundance variations as a function of radius as well as mass segregation, and provide a comparison between the cluster CMD and theoretical isochrones.

The data were all secured at CFHT over two observing seasons: 1984 June and 1985 June. On all nights photometric conditions allowed photometric transfers from the standard stars to be made to the program fields. This will allow us to make an independent comparison between the existing photometry and our new CCD work. The CFHT CCD was used at the prime focus for all the exposures. In this configuration the field size is $2'.2 \times 3'.5$ with each pixel corresponding to $0''.42$. The seeing during the data acquisition ranged from $0''.7$–$0''.9$. A log of the observations is presented in Table 1. In all cases multiple exposures in a given color in the same field were averaged to produce a final frame which was then analyzed. In Table 1 r_{obs} is the radius at which the observations were secured at in units of the core radius (Webbink 1985). The

[1] Visiting Astronomers, Canada-France-Hawaii Telescope. CFHT is operated by the National Research Council of Canada, the Centre National de la Recherche Scientifique of France, and the University of Hawaii.

TABLE 1

JOURNAL OF OBSERVATIONS

Field	r_{obs}	Date	V	B	U
Inner	8	1985 June 9	9 × 300 s	9 × 300 s	1 × 3600 s
Middle	21	1984 June 3	3 × 900 s	3 × 900 s	...
Outer	58	1985 June 10	1 × 900 s	1 × 900 s	1 × 1800 s

inner field is roughly centered on star II-44 of Buonanno, Corsi, and Fusi Pecci (1981), the middle on star P in Zone II of Arp (1962), while the outer field is located at ~25′ due west of the center. Standard stars were selected from Landolt's (1983) equatorial networks and from the M92 photometry of Davis (1985). Flat-fielding was accomplished by exposing on a portion of the dome illuminated with light filtered to match the color of the night sky. With the CFHT RCA CCD camera no defringing is required in U, B, or V. Figures 1–3 display the final averaged V frame for each field.

In the figures illustrating the frames, the stars indicated are the secondary standards defined in each field. The photometry of these stars was determined with respect to the primary standards using aperture photometry and appropriate aperture corrections to account for the different image profiles on the various frames. The transformation equations determined from the primary standards were of the form $(B-V) = 0.391 + 1.298(b-v)$ with a dispersion, σ, equal to ± 0.023, $(U-B) = 0.048 + 0.936(u-b)$ with $\sigma = \pm 0.004$, and $V = v - 0.076(B-V) + 26.482$ and $\sigma = \pm 0.014$. In these equations U, B, and V represent standard magnitudes, and u, b, and v are instrumental magnitudes which normally would be corrected for extinction. The standard star observations were secured, however, at zenith distances within 0.01 air mass of that of the cluster so that extinction corrections in this case were not required. The moderately large color term in $(B-V)$ results from a slight mismatch between the standard bandpass in B and the filter used. Table 2 provides UBV magnitudes for the secondary standards defined in the three fields. No U photometry was secured in the middle field since at the time the data were obtained, no proper filter was available.

The program frames themselves were reduced using DAOPHOT (Stetson 1986), which contains star-finding and profile-fitting routines. Details of the operation of DAOPHOT can be found in Smith *et al.* (1986). In the star-finding routines a detection threshold of 3.5 σ above the sky was used in order to find the objects. A second and a third pass were then made through the data each time after subtracting the located stars out of the frames. Finally, a visual inspection of the subtracted frames allowed stars missed by these multiple automated passes to be included into the stellar coordinate lists. Using this final list of stars, two more passes were made through the data. At this point no new stars were added to the lists, but the first pass allowed some spurious objects to be rejected by the PSF fitting algorithm and the second allowed for larger groups, fewer nonstellar objects, and hence better photometry. When the final photometry was completed a visual inspection of *every* star found on *every* frame was made. All extended objects, possible cosmic rays, or stellar objects badly contaminated by saturation streaks or CCD imperfections were removed from the lists going to make up the CMD of the cluster. However, all stellar objects, even if contaminated, were retained in lists used to make up the cluster luminosity function.

For purposes of economy we will not present lists of the photometry; many thousand entries would be required to do this. If any readers desire such information it will be sent upon request. However, we do provide comparisons of our CCD photometry with the photographic photometry of (1) Arp (1962) and (2) Buonanno, Corsi, and Fusi Pecci (1981). In Table 3 we list our CCD photometry and compare it with the photometry of Arp (1962) from his Zone II. All entries denoted by footnote (a) are photolectric standards used by Arp to calibrate his photographic data. In the table the X, Y coordinates are those from our middle field, the magnitudes and colors are from our CCD photometry, while the differences are in the sense of CCD–Arp. While it is clear that there are some large differences for the stars fainter than $V = 20.5$, for those brighter than this limit the agreement is excellent. The mean difference in V for these nine brightest stars is 0.03 ± 0.05, and that in $(B-V)$ is 0.01 ± 0.09. Table 4 provides a comparison between the present CCD photometry of the inner field and

TABLE 2

SECONDARY PHOTOMETRIC STANDARDS

Field	X, Y	V	$B-V$	$U-B$
Inner	307, 341	17.097	0.723	0.029
Inner	257, 342	14.997	0.390	0.245
Inner	222, 368	15.360	0.028	−0.130
Inner	177, 255	15.781	0.806	0.151
Inner	149, 319	16.322	−0.128	−0.495
Inner	64, 49	15.195	0.092	0.001
Inner	42, 137	15.688	0.845	0.216
Middle	295, 79	20.503	−0.089	...
Middle	269, 368	17.521	1.287	...
Middle	233, 123	18.645	0.473	...
Middle	141, 142	20.616	0.711	...
Middle	130, 69	18.189	0.457	...
Middle	106, 162	18.905	0.456	...
Middle	92, 19	18.475	1.399	...
Middle	74, 161	18.766	0.463	...
Outer	287, 172	16.790	0.716	0.257
Outer	203, 447	17.817	1.533	...
Outer	67, 197	16.417	0.612	0.060

TABLE 3

COMPARISON OF CCD PHOTOMETRY WITH PHOTOMETRY OF ARP

Arp Name	X, Y	V	$B-V$	ΔV	$\Delta(B-V)$
e[a]	152, 268	19.67	0.58	−0.01	−0.02
p[a]	188, 206	17.59	0.61	0.02	−0.06
435	220, 107	20.06	0.61	0.05	−0.08
439[a]	84, 65	20.75	0.57	0.27	−0.20
467	206, 136	20.64	0.87	0.06	0.08
468	200, 151	20.38	0.60	0.07	−0.01
471	141, 142	20.62	0.60	0.24	−0.09
472	165, 91	21.45	0.70	0.87	−0.16
473[a]	73, 117	20.64	0.59	0.20	−0.18
489	246, 285	20.51	0.70	−0.10	0.21
491	218, 273	20.30	0.56	−0.02	0.07
494	168, 203	20.44	0.59	0.01	0.10
495	168, 184	20.59	0.68	0.10	−0.10
496	169, 174	21.16	0.72	0.16	−0.08
497	123, 183	20.52	0.53	0.22	−0.20
498	112, 187	19.95	0.61	−0.03	0.18
503	117, 258	19.92	0.48	0.10	−0.09
507	32, 162	20.59	0.59	0.14	−0.14
508[a]	16, 150	20.40	0.62	0.12	0.01
56′	234, 150	21.04	0.67	0.32	−0.21
67′	131, 122	21.66	0.96	0.00	−0.48

[a] Photoelectric standards used by Arp to calibrate his photographic data.

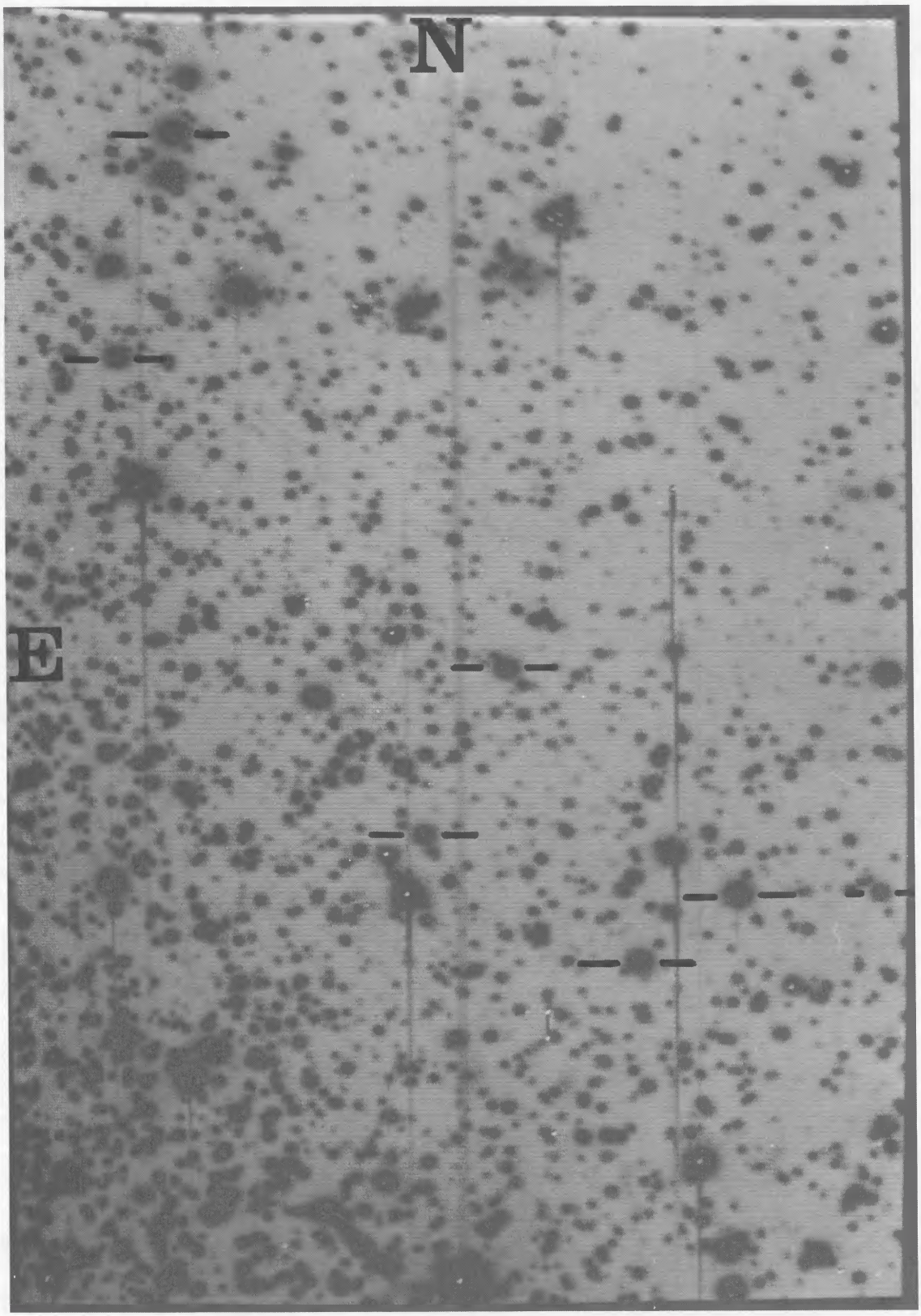

FIG. 1.—*V* CCD frame of the inner field in M5 with the secondary standards marked. The frame shown is an average of the nine exposures obtained and measures ~3.'5 N-S by 2.'2 E-W. Pixel (0, 0) is located in the NE corner, and pixel numbers increase to the south (*Y* pixels) and west (*X* pixels).

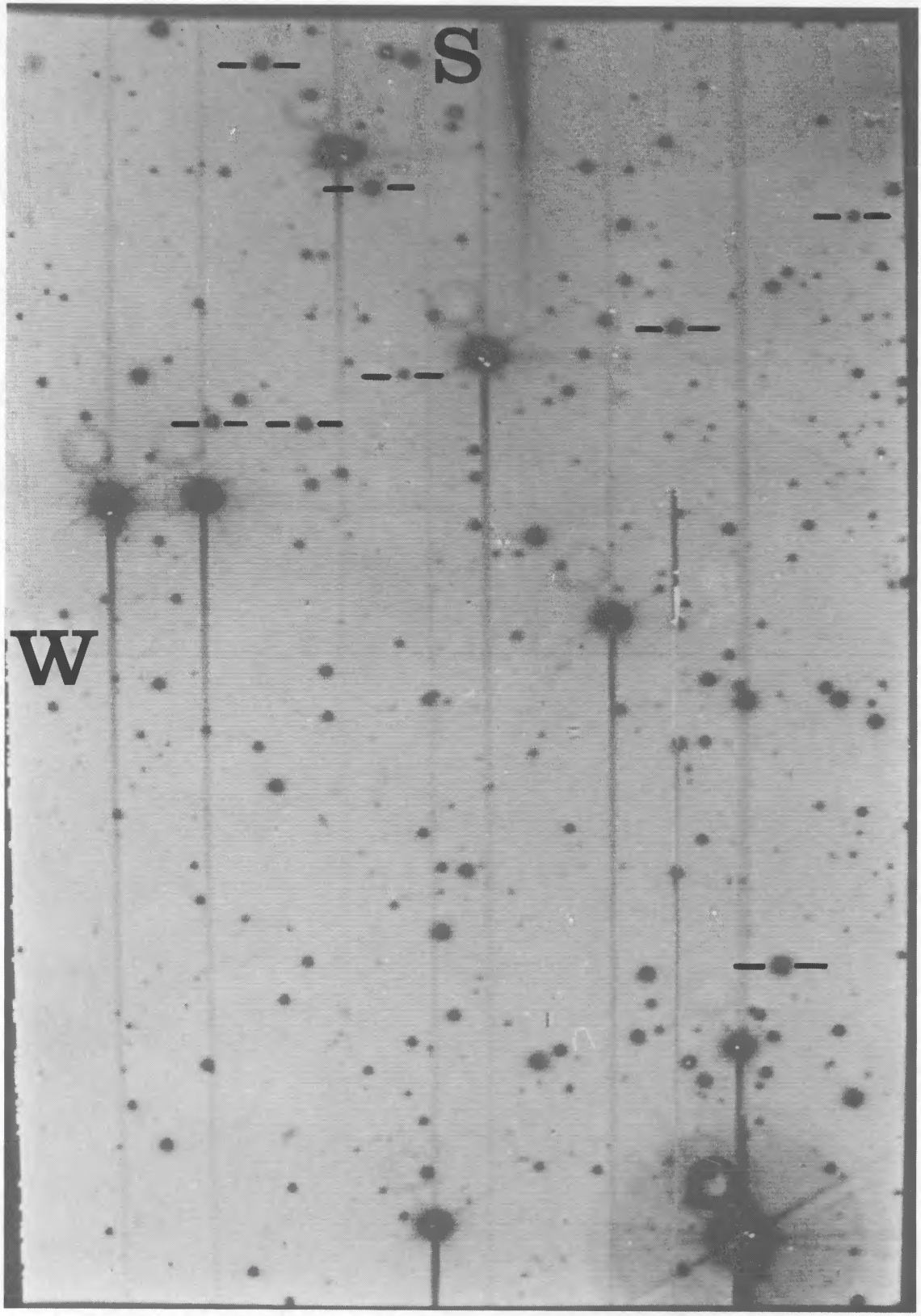

FIG. 2.—*V* CCD frame of the middle field in M5 with the secondary standards marked. The frame shown is an average of the three exposures obtained and measures ~3'.5 N-S by 2'.2 E-W. Pixel (0, 0) is located in the SW corner, and pixel numbers increase to the north (*Y* pixels) and east (*X* pixels).

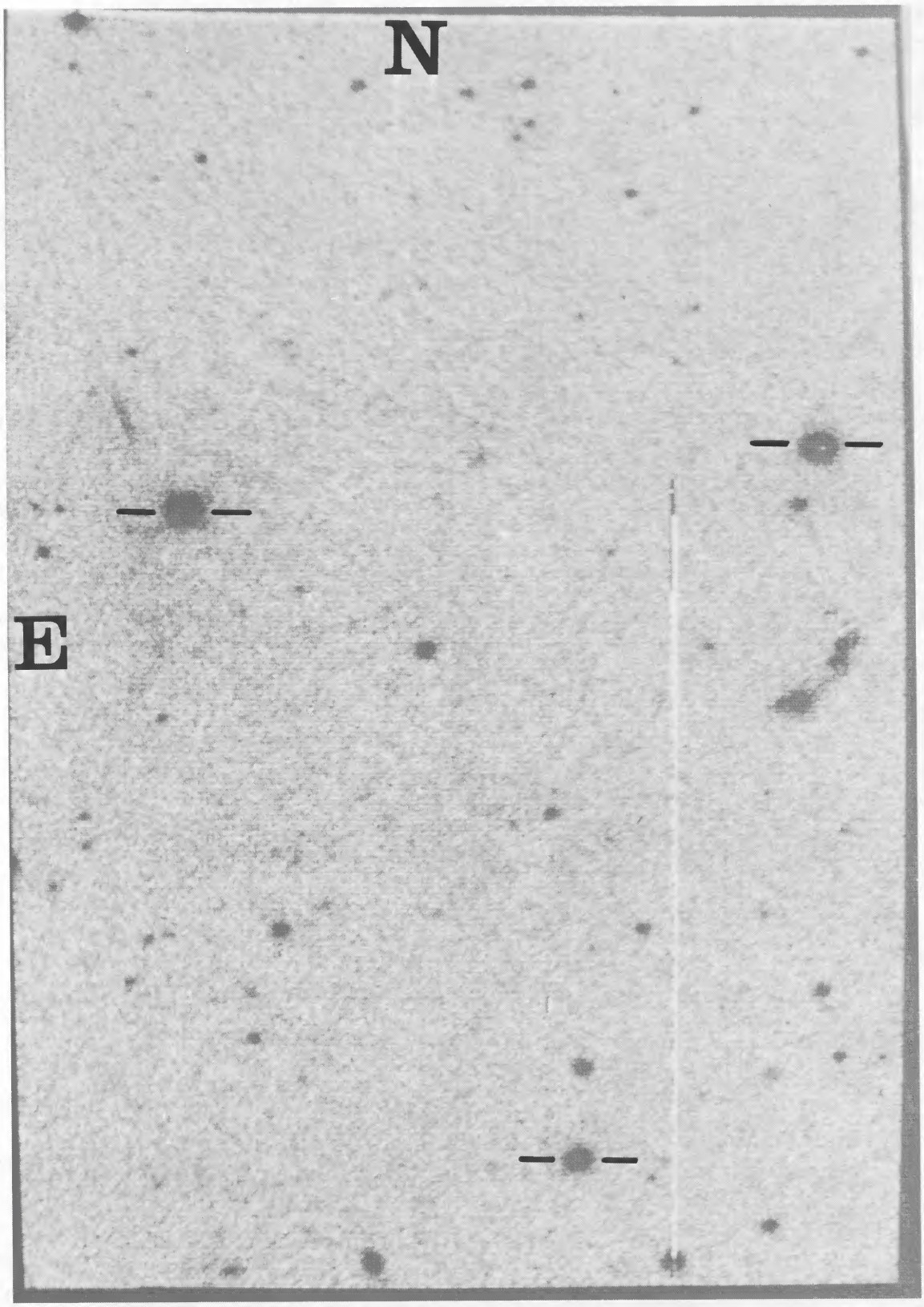

FIG. 3.—*V* CCD frame of the outer field in M5 with the secondary standards marked. The frame shown is a single 900 s exposure and measures ~3'.5 N-S by 2'.2 E-W. Pixel (0, 0) is located in the NE, corner and pixel numbers increase to the south (*Y* pixels) and west (*X* pixels).

TABLE 4

COMPARISON OF CCD PHOTOMETRY WITH THAT OF BUONANNO, CORSI, AND FUSI PECCI

BCF NAME	X, Y	V	B−V	ΔV	Δ(B−V)
II-15	222, 368	15.37	−0.01	−0.13	0.05
II-16	258, 342	14.97	0.87	−0.10	0.08
II-42	114, 267	15.49	0.80	−0.08	0.06
II-43	177, 255	15.79	0.79	−0.08	0.00
II-44	149, 116	15.16	0.56	0.04	−0.02
II-46	64, 49	15.20	0.05	−0.04	0.05
II-47	70, 25	16.24	0.80	0.03	0.05
II-48	43, 102	15.72	0.84	0.06	0.12
II-49	42, 137	15.69	0.85	−0.06	0.03
II-102.....	140, 243	16.53	0.76	−0.09	0.15
II-115.....	298, 62	15.59	0.80	−0.10	0.03
II-124.....	311, 125	15.55	0.79	−0.13	0.01

that of Buonanno, Corsi, and Fusi Pecci (1981). In this case the comparison is less satisfactory with a mean difference in V of -0.06 ± 0.07 and in $(B-V)$ of 0.05 ± 0.05. We seem to be measuring the stars somewhat brighter and redder than the above authors. A possible reason for this difference may be that at only $\sim 4'$ from the cluster center scattered light may be affecting the photographic data more seriously than the CCD data. Evidence that it is the photographic data which is most probably affected comes from the result that our fiducial sequences for the inner and middle fields are identical to within ~ 0.002 mag in $(B-V)$ (see § II).

II. THE COLOR-MAGNITUDE DIAGRAM

a) The V, (B−V) Diagram

In Figures 4 and 5 we present the V, $(B-V)$ CMDs for the inner and middle fields. The outer field has too few stars in it to generate a proper CMD. These diagrams do not contain all the stars measured in each field but are a sample selected to have small errors in the photometry. The initial aim here is just to establish the fiducials for each field and investigate the morphology of the CMDs so that a selected sample is appropriate. The stars were chosen in the following unbiased manner. After the photometry was completed, error curves were constructed from the data using all the stars found. For the errors in the measurements we used the values returned by DAOPHOT, but these were checked by the procedure of adding stars of known magnitude into the frames and rereducing the data in the normal manner. In general, there was good consistency between these two error estimates. Error curves in V for the inner and middle fields are shown in Figures 6 and 7. We then selected only those stars which had an error within 1.5 σ of the median value of the error for its magnitude. After this selection process, the stars on the frames of the same field but with different colors were merged together after registering the frames. A rather small merge radius (1.0 pixel) was used for this process, again selecting further for stars with the best photometry. As an example of this process, in the inner field 2542 stars were measured on the V frame and 2532 on the B frame.

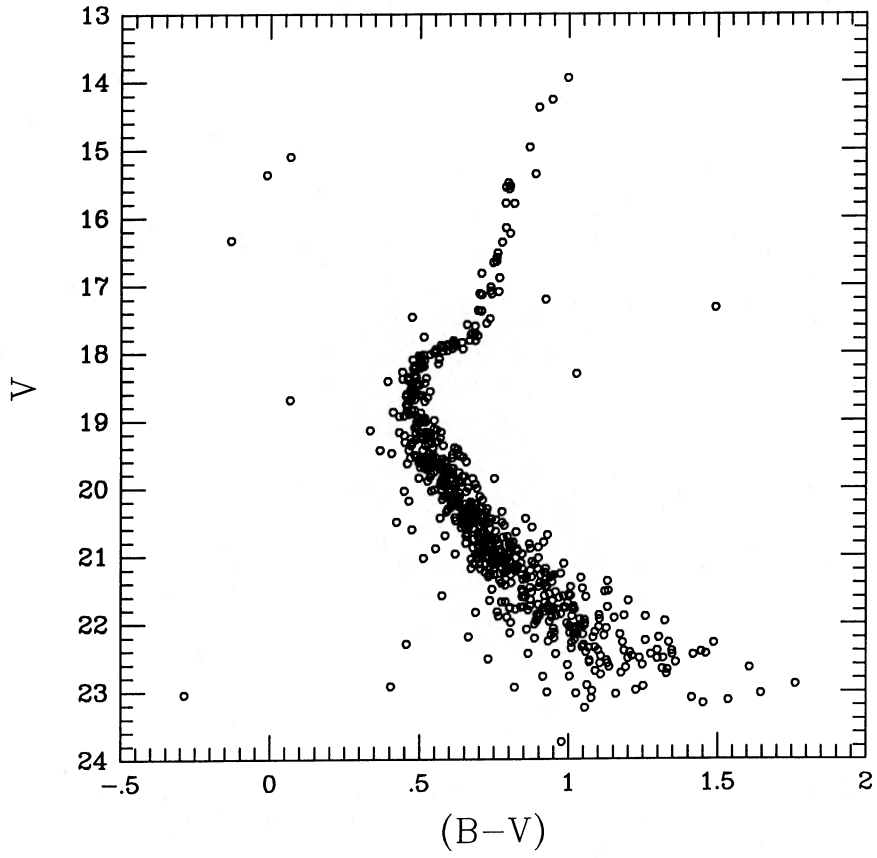

FIG. 4.—The color-magnitude diagram for the inner field. The points plotted have been selected to have small errors in the photometry and represent only ~25% of all the stars in the frames.

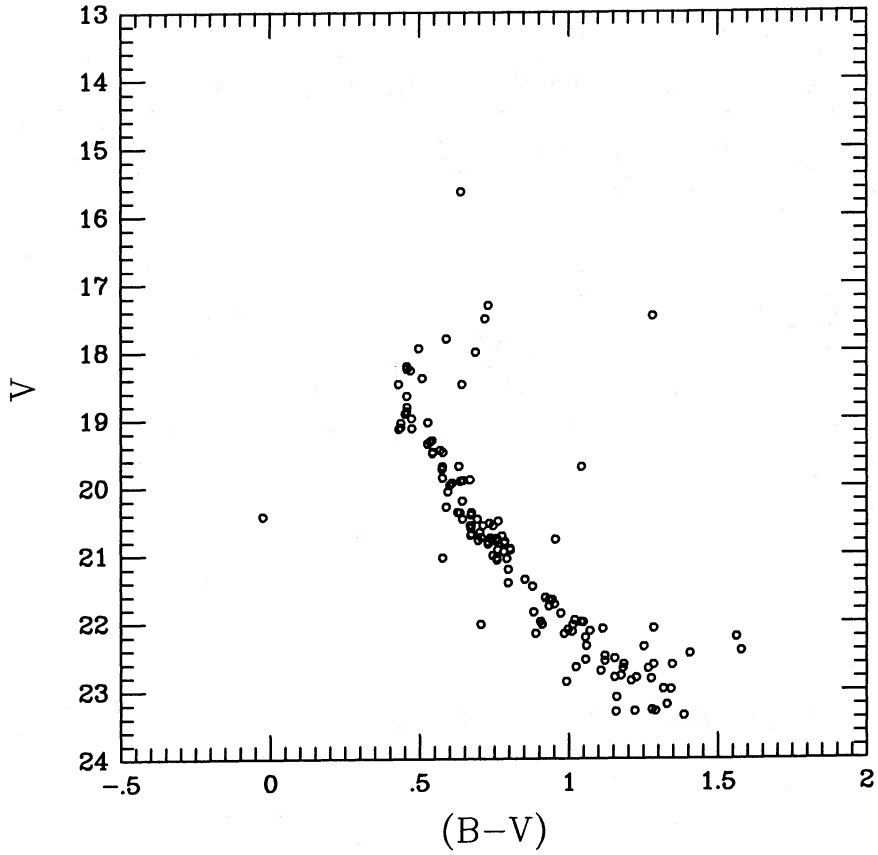

FIG. 5.—The color-magnitude diagram for the middle field. The points plotted have been selected to have small photometric errors and represent only ~20% of all the stars in the frames.

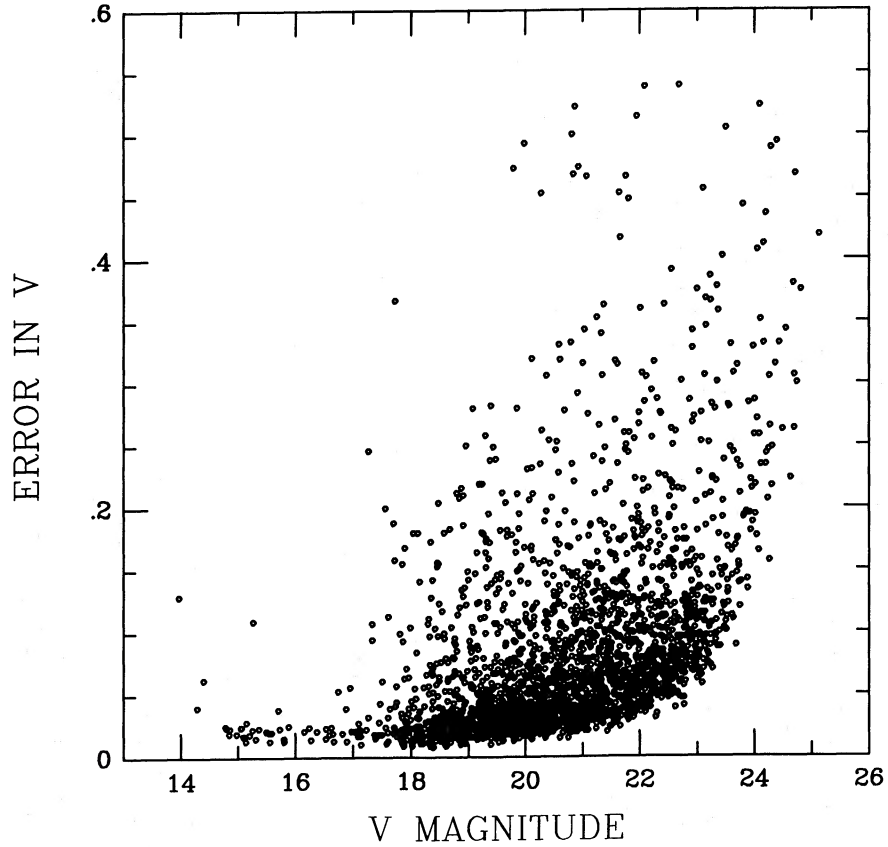

FIG. 6.—The error in the V magnitude for stars in the inner field

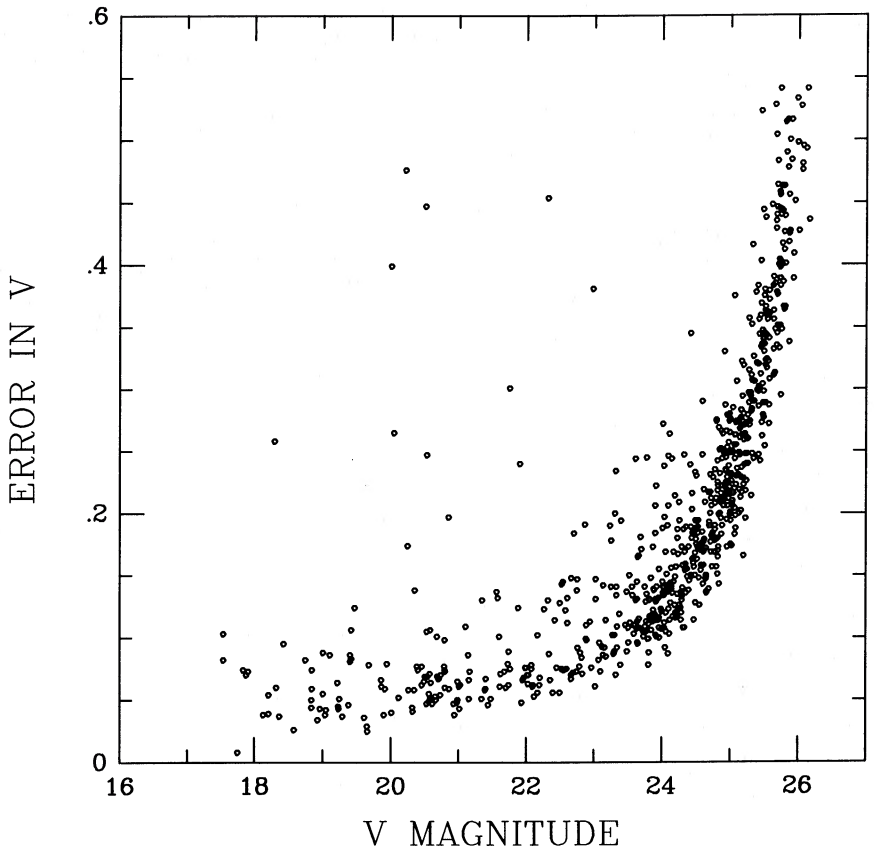

FIG. 7.—The error in the V magnitude for stars in the middle field

In the CMD for this field (Fig. 4) only 688 stars are contained in the diagram.

Several results of interest are clear from a simple inspection of the cluster CMDs. (i) The bluest extension of the main sequence is not sharply defined, but the turnoff is nearly vertical between $V = 18.2$ and 19.0. It is thus difficult to define precisely the magnitude difference between the horizontal branch and the turnoff, a quantity that is related to the cluster's age (Sandage 1982). This vertical morphology of the turnoff is a common feature in intermediate metallicity clusters (Smith *et al.* 1986). The horizontal branch of M5 is located at $V = 15.11$ (Arp 1962) so that the difference in V magnitudes between it and the turnoff is ~ 3.5 if the middle of the vertical extent of the turnoff region is adopted as the bluest point. This is entirely typical of other clusters (Sandage 1982), but the error of ± 0.2 mag in this quantity translates to an uncertainty in the age of the cluster of ± 3 Gyr (Smith *et al.* 1986; Sandage 1982). (ii) There is no evidence for a binary sequence composed of approximately equal mass binaries in either field of M5. (iii) In neither field is there any obvious blue straggler population. (iv) In the inner field there is one very good candidate cluster white dwarf at $V = 23.04$ ($M_V = 8.7$), $(B-V) = -0.29$. An estimate of the number expected can be obtained as follows. Using the simple analytic King model approximation (King 1962) and the parameters tabulated by Peterson and King (1975), we calculate that the total luminosity sampled in our CCD field is $L_T = 1.2 \times 10^4\ L_\odot$. Using the Bahcall-Soneira luminosity function (see Bahcall 1985), we estimate that we would expect to see 8.6×10^3 stars in our inner field down to $M_V = 9.7$ ($V = 24.0$). In fact, we find 5.6×10^3 (see Tables 8 and 9) down to this limit, or $\sim 65\%$ of the predicted number. In view of the approximations which go into this calculation, this level of agreement is entirely satisfactory. The white-dwarf population is determined using the equation developed by Renzini (1985): $N_{\rm WD}(<M_V) = 4.7 \times 10^{-11} \times L_V \times t_C(M_V)$, where L_V is the visual luminosity and t_C is the time for a white dwarf to reach M_V. Following the discussion of Renzini (1985), we assume that $L_V = 0.5 L_T = 6.2 \times 10^3\ L_\odot$ and calculate that $t_C = 9.0 \times 10^7$ yr for a white dwarf to reach $M_V = 9.7$. From this we obtain our prediction of $N_{\rm WD}$ ($<M_V = 9.7$) = 26 in the inner field. This could be reduced to 17 if the correction of 0.65, based on the observed to calculated star counts, is applied. The completeness factor at the faint limit in this field is 12.0 (see § V), hence we would expect to observe only one or two cluster white dwarfs, which is consistent with our result. Note that it is the crowding which is limiting the detection. In view of the good seeing we enjoyed at CFHT, it would seem very difficult to improve upon the data in a single field. It does, however, seem very likely that a significant number of white dwarfs could be detected from the ground by observing multiple fields arranged in annuli about the cluster center.

b) *The Cluster Fiducial Sequences at Different Radii*

Fiducial sequences were constructed from the data contained in Figures 4 and 5 by binning stars over 0.2 mag intervals in V and determining the mean in $(B-V)$ for each bin. Obvious field stars were excluded from this process. The resulting sequences are listed in Table 5. It is important to realize that the data entering into these fiducials were secured a year apart and were calibrated entirely independently. The

TABLE 5

FIDUCIAL SEQUENCES FOR INNER AND MIDDLE FIELD

$V(\pm 0.10)$	Inner $(B-V)$	Middle $(B-V)$	$V(\pm 0.1)$	Inner $(B-V)$	Middle $(B-V)$
13.9.....	0.997	...	19.5	0.556	0.549
14.3.....	0.923	...	19.7	0.557	0.594
14.9.....	0.868	...	19.9	0.605	0.623
15.3.....	0.889	...	20.1	0.617	0.619
15.5.....	0.798	...	20.3	0.665	0.644
15.7.....	0.803	...	20.5	0.693	0.704
16.1.....	0.789	...	20.7	0.730	0.727
16.3.....	0.791	...	20.9	0.760	0.777
16.5.....	0.761	...	21.1	0.784	0.775
16.7.....	0.753	...	21.3	0.856	0.838
16.9.....	0.738	...	21.5	0.909	0.842
17.1.....	0.729	...	21.7	0.924	0.951
17.3.....	0.703	...	21.9	0.970	0.979
17.5.....	0.707	0.719	22.1	1.013	1.016
17.7.....	0.683	...	22.3	1.107	1.123
17.9.....	0.605	0.600	22.5	1.213	1.165
18.1.....	0.512	...	22.7	1.189	1.236
18.3.....	0.480	0.473	22.9	1.200	1.278
18.5.....	0.482	...	23.1	1.255	1.249
18.7.....	0.479	0.458	23.3	...	1.304
18.9.....	0.478	0.459	23.5	...	1.476
19.1.....	0.509	0.468	23.7	...	1.469
19.3.....	0.516	0.530	23.9	...	1.417

fiducials presented have not been smoothed, so small number statistics will cause some scatter in the tabulated sequence. The two fiducials are plotted together in Figure 8, and it is clear from this diagram and Table 5 that the sequences are virtually identical. Formal comparisons imply that any difference between the two sequences are at the level of 0.002 mag in $(B-V)$ at a given V through the unevolved part of the main sequence where the stellar densities are high enough to define a statistically valid sequence. This excellent agreement between the two fiducials provides confidence in their location in the CMD and leads to the conclusion that the systematic difference seen in the inner field CMD between the current CCD work and that of Buonanno, Corsi, and Fusi Pecci (1981) is likely due to a small systematic error in the photographic diagram.

This very small difference (which is fully consistent with no difference at all) between the two fiducials also sets an upper limit to any gross metal abundance difference in the two fields in M5. In our M13 paper (Richer and Fahlman 1986) we showed that the VandenBerg and Bell (1985) isochrones could be used to estimate any small chemical inhomogeneities among main-sequence stars by examining the widths of cluster main sequences and assuming that any intrinsic width is due to chemical inhomogeneity. The same principle applies here to the location of the sequence itself and, assuming constant Y between the two fields, we can derive that there is no *gross* metal abundance difference between a field in M5 at 8 core radii from the center and one at 21 core radii larger than 4%.

The importance of this result is that it is well known that elliptical galaxies and the spheroidal component of spirals do often show radial color and absorption-line gradients. These have usually been interpreted as metal abundance gradients which, if correct, probably reflect metal formation processes in

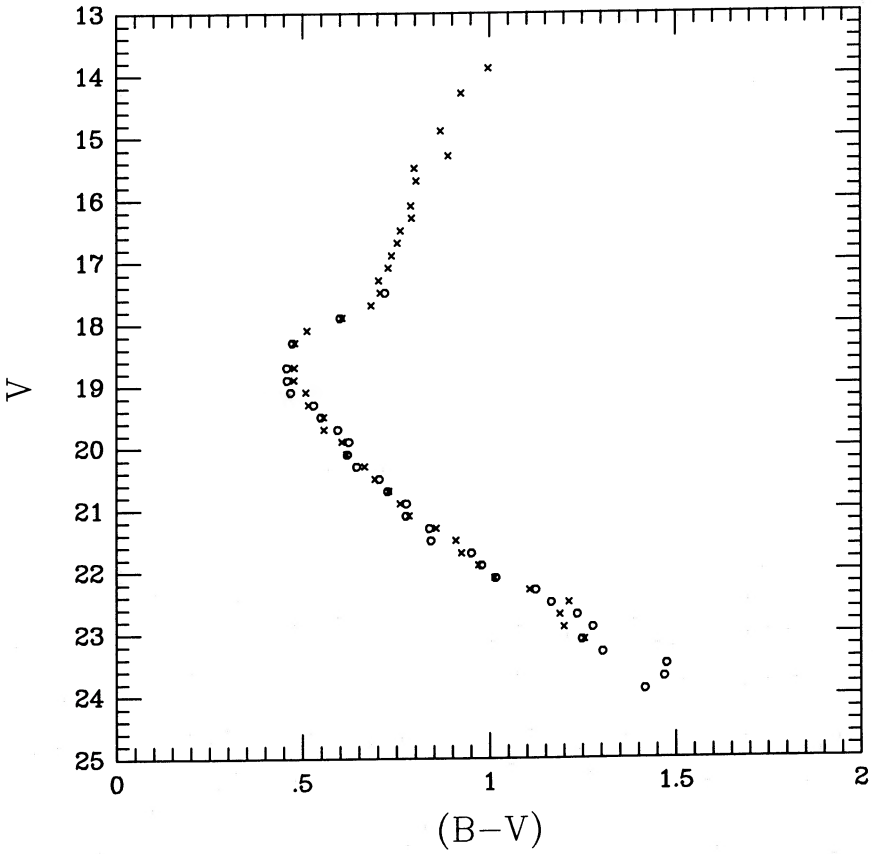

FIG. 8.—The color-magnitude diagram fiducials for the inner field (*crosses*) and the middle field (*open circles*). No smoothing was applied to these fiducials.

the early stages of galactic evolution. With globulars, however, the usual assumption is that they are chemically homogeneous, reflecting the abundance of the gas out of which they formed. While there is certainly evidence that a few globulars have appreciable chemical inhomogeneity and that some show radial color gradients (Chun and Freeman 1979; Peterson 1986), those that only exhibit color gradients are probably just reflecting the random statistical distribution of the bright stars (Peterson 1986). The result found here certainly is consistent with that interpretation and sets the most stringent upper limit yet on any radial chemical abundance variation in a globular.

c) *The $U, (U-V)$ Color-Magnitude Diagram*

In Figure 9 we plot the U, $(U-V)$ CMD for stars in the inner field. This diagram will likely be of interest to those planning Hubble Space Telescope observations of globulars as this filter combination is expected to be a popular one with that instrument. Since a deep diagram in these colors has never been published for any globular, we describe the morphology of it for M5 and compare it with that for a more metal rich and more metal poor cluster. In the M5 diagram the horizontal branch occurs at $U \approx 15.6$ and appears to dive steeply to faint magnitudes for stars with $(U-V) < -0.5$. In fact, there appears to be a continuation from the horizontal branch region down toward the white-dwarf area. This morphology is not seen in the $V, (B-V)$ CMD of Arp (1962) where the horizontal branch seems completely truncated at $V = 16.5$ ($U = 15.7$). The white-dwarf candidate discussed in § II does not appear in Figure 9 since it falls on a bad pixel on the U frame. The red giant branch is well defined and very narrow in the diagram, with no evidence of an asymptotic giant branch (AGB). The subgiant branch is very flat in U over a range in $(U-V)$ of ~ 0.3 mag at $U = 18.4$. We will have more to say about this feature shortly when we compare this M5 diagram with that of a more metal poor and metal rich cluster. The turnoff is sharply defined at $U = 18.4$, but this does not appear to be the bluest extension of the main sequence, which occurs at about $U = 19.2$. The lower main sequence is well defined and tightly delineated to the limit of the photometry at $U = 23$.

Figure 10 compares fiducial sequences in the $M_U, (U-V)_0$ plane for three clusters of very different metallicities. The clusters are M15 with the data taken from Fahlman, Richer, and VandenBerg (1985), M5, and M71 (Richer and Fahlman 1987). Adopted properties of these clusters are tabulated in Table 6. The main points of interest in this comparison are as follows. (1) The absolute magnitude of the turnoff decreases by ~ 0.5 mag in going from the metal-poor cluster ($[M/H] = -2.15$) to

TABLE 6

PROPERTIES OF CLUSTERS

Cluster	$[M/H]$	$(m-M)_V$	$(m-M)_U$	$E(U-V)$	Reference
M15.....	−2.15	15.4	15.6	0.20	1, 2
M5	−1.13	14.3	14.4	0.05	3
M71.....	−0.58	13.7	14.2	0.50	1, 4

REFERENCES.—(1) Zinn and West 1984; (2) Fahlman, Richer, and VandenBerg 1985; (3) this paper; (4) Richer and Fahlman 1987.

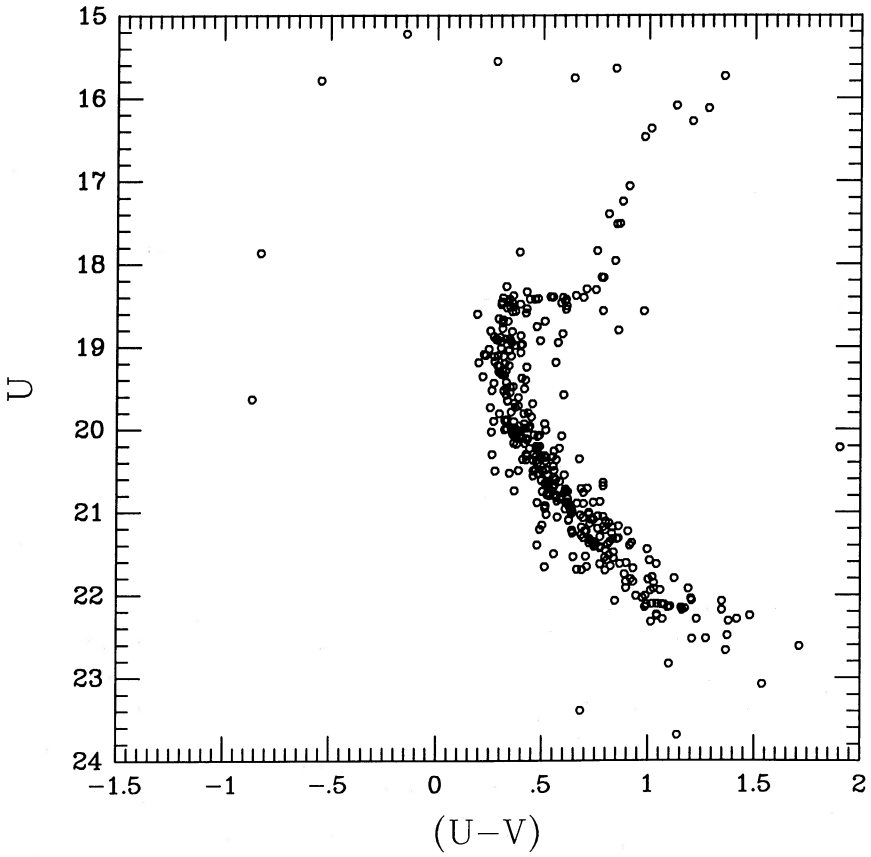

FIG. 9.—The $U, (U-V)$ color-magnitude diagram for stars in the inner field

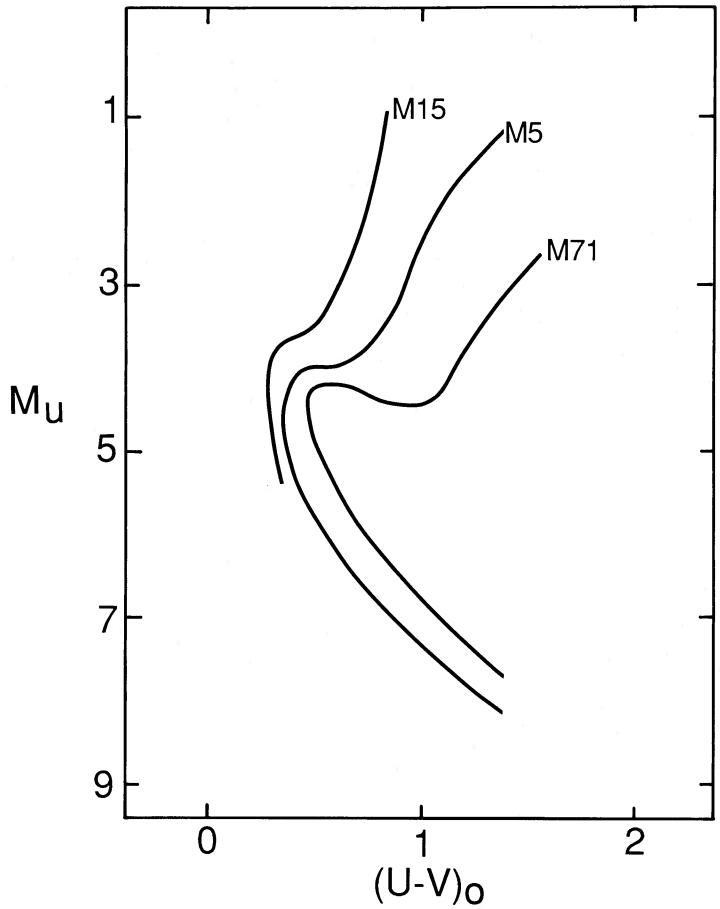

FIG. 10.—Fiducial sequences in the M_U, $(U-V)_0$ plane for three globular clusters with different metal abundances; M15 ([M/H] = −2.15), M5 ([M/H] = −1.13), and M71 ([M/H] = −0.58).

a metal-rich one ([M/H] = −0.58) (2) Although the M15 diagram does not go very deep, it seems clear from Figure 10 that there is a clean separation between the positions of the lower main sequences of the three clusters. Fainter than M_U = 6, where evolutionary effects are expected to be unimportant, the M5 and M71 lower main-sequence loci are separated by 0.5 mag in M_U. (3) The subgiant branch in M15 is very short and slopes slightly upward, while that for M5 is well defined and flat for ∼0.3 mag in $(U-V)$. The M71 subgiant branch extends for over 0.5 mag in $(U-V)$ and is generally sloped downward. (4) The positions of the giant branches are widely separated for the different metal abundances. As expected, the more metal poor the cluster, the bluer the location of the giant branch. The termination points of the red giant branches should *not* be taken from Figure 10, since small number statistics has not allowed us to define the true tip of the red giant branches.

III. THE FUNDAMENTAL PARAMETERS FOR M5

a) Reddening

The reddening in the direction of M5 has been shown to be very small. Arp (1962) derived that $E(B-V)$ was essentially zero, while Harris and Racine (1979) give 0.03. Recently Burstein, Faber, and Gonzalez (1986) showed that it should not exceed 0.03 mag. In Figure 11 we display the color-color diagram based on data from the inner field. There are two horizontal branch stars in this diagram which can be used to establish a value of the reddening. The brighter star yields $E(B-V) = 0.00$ while the fainter one results in 0.04. Between these values and those already existing in the literature, we will adopt $E(B-V) = 0.02$ for M5.

b) Metal Abundance

The metal abundance of M5 has been reported to be anywhere from [M/H] = −0.68 (Osborn 1971) to −1.59 (Zinn 1980; see Burstein, Faber, and Gonzalez [1986] for a recent summary of metal abundance determinations in M5). We can provide some input by obtaining a value of $\delta(U-B)_{0.6}$, the ultraviolet excess of the main-sequence stars at $(B-V)_0 = 0.6$ which is known to be correlated with metal abundance (Wallerstein and Carlson 1960; Wallerstein 1962; Sandage 1969, 1970; Carney 1979). From Figure 11, with a reddening of 0.02 mag, and using the Hyades fiducial sequence, we derive that $\delta(U-B)_{0.6} = 0.18$ with an error of ±0.02 mag. This is somewhat smaller than the value of 0.21 derived by Arp (1962).

The relation between $\delta(U-B)_{0.6}$ and [M/H] remains somewhat ill-defined for globular clusters. In our M4 (Richer and Fahlman 1984) and M13 (Richer and Fahlman 1986) papers we attempted to define a relation between these parameters. The correlation discussed in the M13 paper was between $\delta(U-B)_{0.6}$ and metallicities derived from infrared observations (Frogel, Cohen, and Persson 1983), and M5 was itself a cali-

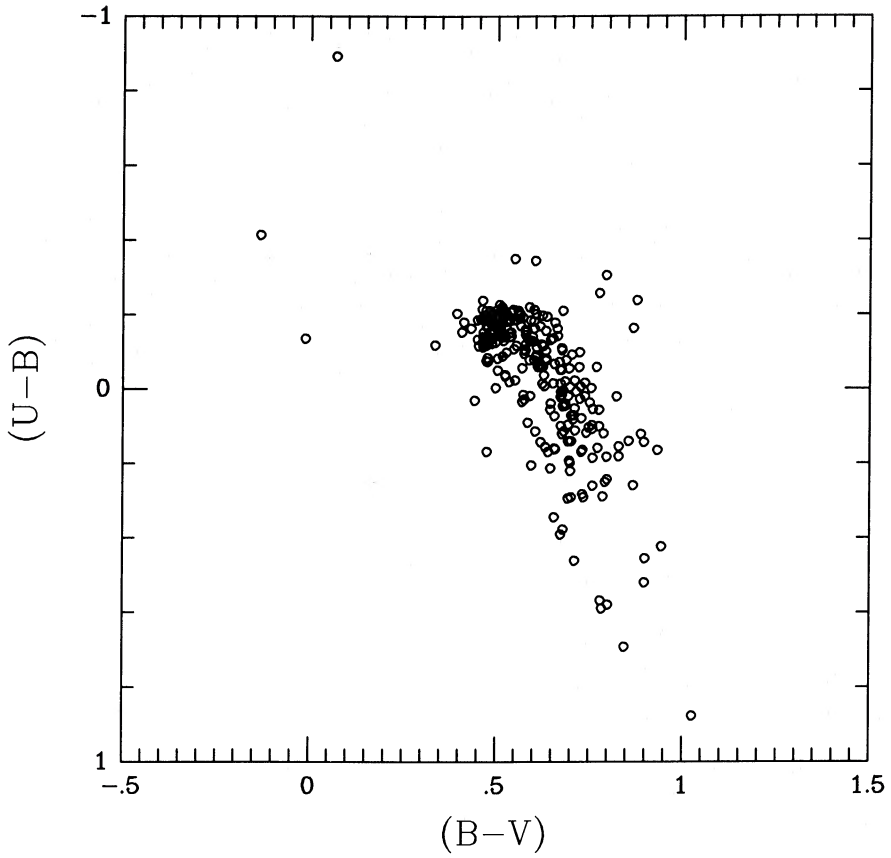

FIG. 11.—Color-color diagram for stars in the inner field

brator of this relation. If we use this relation to obtain a value of $[M/H]$ for M5 from its value of $\delta(U-B)_{0.6}$, we derive that $[M/H] = -1.13(\pm 0.11)$. This is in good agreement with several recent estimates from both low and high resolution studies (see Burstein, Faber, and Gonzalez 1986), and we adopt this value in the ensuing discussion.

c) *The Distance to M5*

In our earlier papers we have been deriving distances to globulars by fitting a small sample of subdwarfs to the lower main sequences of these clusters, in much the same way that distances to galactic open clusters are arrived at by fitting to the Hyades. There has been some uncertainty in this approach as to whether the statistical Lutz-Kelker (1973) corrections should be applied to the subdwarfs. Recent discussions with T. Lutz have convinced us that the full Lutz-Kelker corrections are much too large, and a more realistic approach would be to neglect them entirely. We had suspected this for some time (see comments in Richer and Fahlman 1986), since distances derived without these corrections always agreed better with the theoretical isochrones.

If we use the subdwarfs listed in Fahlman, Richer, and VandenBerg (1985) with no Lutz-Kelker corrections and correct their $(B-V)$ colors so that they represent stars with the metal abundance of M5 (see Fahlman, Richer, and VandenBerg 1985) and apply the reddening correction of 0.02 mag, the best fit between the subdwarfs and the M5 fiducial occurs for an apparent distance modulus of 14.30. The formal error in this determination is ± 0.2 mag.

We have now determined the distances to four globulars with a good range in metal abundance using the subdwarfs to fit the lower main sequences of the clusters. It is of some interest to investigate the location of the horizontal branch in these clusters when the distances are calibrated in this manner. Table 7 presents these data. It should be kept in mind that the distances listed in this compilation used no Lutz-Kelker corrections. The observed locations of the horizontal branches were taken from Harris and Racine (1979). As already noted by Sandage (1982), there is a clear correlation between the metal abundance of the cluster and the luminosity of the horizontal branch.

IV. THE AGE OF M5

We derive an age for M5 by *overlaying* the VandenBerg and Bell (1985) isochrones on the CMD fiducials of M5. All the cluster parameters except the helium abundance and the mixing-length parameter have been fixed by the observations, and the values adopted for these latter two quantities are

TABLE 7

DISTANCES AND HORIZONTAL BRANCH LOCATIONS

Cluster	$[M/H]$	$(m-M)_V$	V(HB)	M_V(HB)
M15.....	−2.15	15.42	15.86	0.44
M13.....	−1.40	14.39	14.95	0.56
M5	−1.13	14.30	15.11	0.81
M4	−0.93	12.50	13.33	0.83

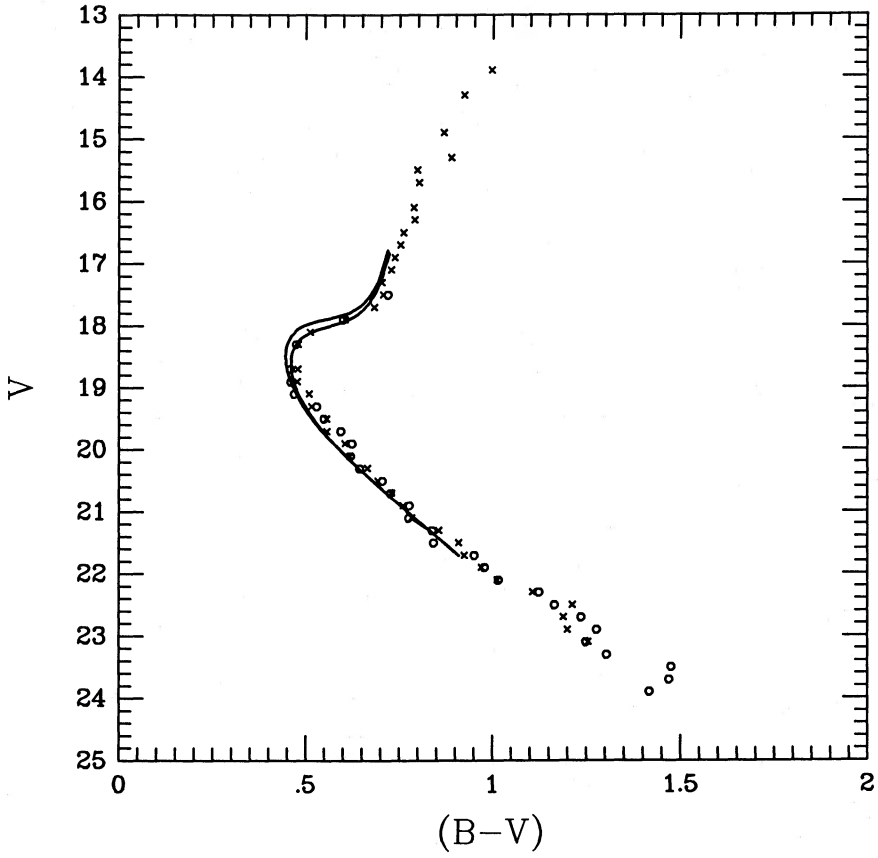

FIG. 12*a*

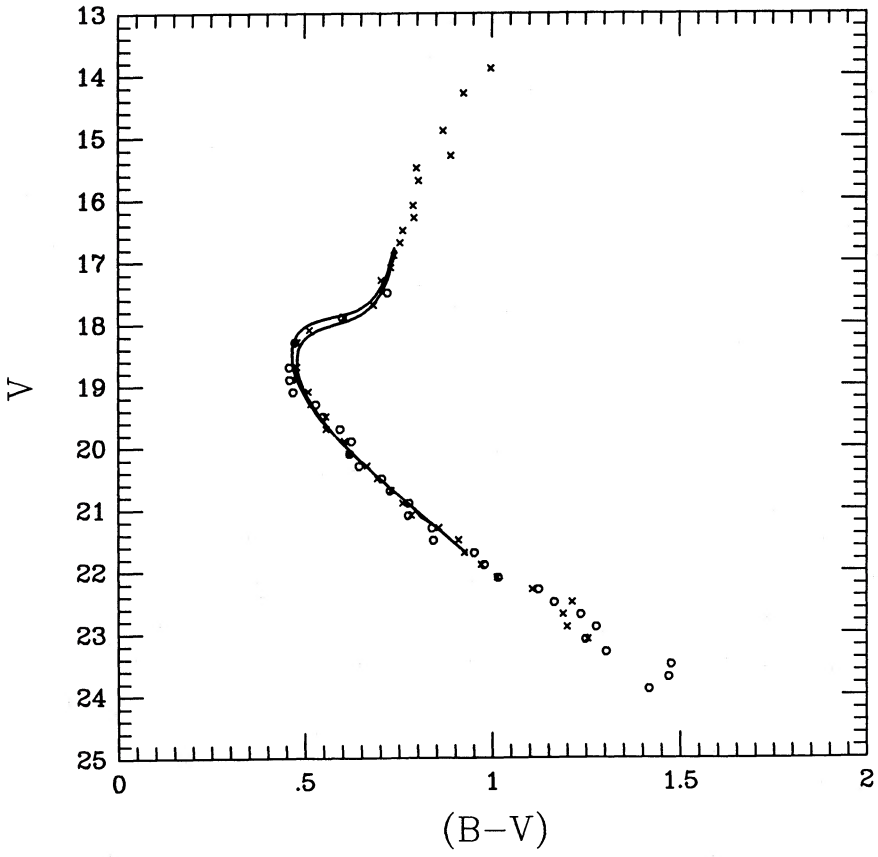

FIG. 12*b*

FIG. 12.—(*a*) Isochrones from VandenBerg and Bell (1985) for 16 and 18 Gyr, $Y = 0.2$, $[M/H] = -1.1$, and $\alpha = 1.6$, are shifted so that they represent a cluster with $(m-M)_V = 14.3$ and $E(B-V) = 0.02$ and are then overlaid on the M5 fiducials from Fig. 8. No further shifting is carried out. Hence Fig. 12 can be used to evaluate the good agreement between the cluster data and the theoretical calculations. (*b*) Same as (*a*) except that the isochrones have been shifted redward by 0.02 mag in $(B-V)$. This figure is then used to derive an age of 17 Gyr for M5.

$Y = 0.20$ and $\alpha = 1.6$. Our derived metal abundance for M5 falls about midway between grid points in the $[M/H]$-space calculated by VandenBerg and Bell so that we were required to interpolate a set of isochrones appropriate to $[M/H] = -1.1$. These isochrones for ages of 16 and 18 Gyr, overlaid on the fiducials for the inner and middle fields discussed in § II, are displayed in Figure 12*a*.

It is apparent that the lower main sequence ($V > 20.5$) is well matched by the isochrones, but in the region between $V = 20.5$ and $V = 18.5$ the cluster fiducials are somewhat redder than the theoretical calculations. In the region of the subgiants, the theory and observations are in good agreement for an isochrone of 18 Gyr, while the observed giant branch appears redder than the theoretical branch. Overall, the 18 Gyr isochrone is a much better fit to the data than that for 16 Gyr. As a general point, because all the cluster parameters with the exception of Y and α were determined observationally, Figure 12*a* can be taken as a measure of the current excellent accord between observed locations of cluster CMDs and theory for ages in the range of 16–18 Gyr. However, in order to determine a proper age for a cluster, it is essential that the turnoff data be well centered by the theoretical loci; otherwise the derived age is likely to be incorrect. In Figure 12*a*, for example, it does appear that the isochrones are on the blue side of the observations. If we apply a redward shift of 0.02 mag in $(B-V)$, a much superior fit is obtained. This is illustrated in Figure 12*b*. Such a small shift seems justified when we consider possible errors in the conversion from the theoretical plane to the observer's, errors in the zero point of the photometric calibration, the reddening, and metal abundance of the cluster. From Figure 12*b* we can derive an age of $17(\pm 1)$ Gyr for the age of M5, and we take this as our best estimate. With the data seen in Figure 12*b*, it is difficult to imagine a value of the Hubble constant H_0 near 100 km s^{-1} Mpc^{-1} with conventional cosmologies, unless there is a non zero cosmological constant.

V. THE LUMINOSITY FUNCTIONS

In this section we derive the luminosity functions for M5 in the three radial fields. Since the V frames reached deeper than those in B in all the fields surveyed, we adopt the following procedure in deriving the luminosity functions. (1) All stars present on the V frames at a level of at least 3.5 σ above the sky are initially counted. (2) Corrections for incompleteness are determined by adding stars into the frames and rereducing them again in the normal fashion. (3) The field star contribution is evaluated from published theoretical models of star counts (Bahcall and Soneira 1980). Unfortunately, no blank fields were measured for M5, but this is not a serious limitation since the cluster is at high galactic latitude where the field star contamination is modest. The results of the incompleteness corrections are listed in Table 8. For the inner field a total of 465 stars were added into the V frame in six trials, while the equivalent numbers for the middle field are 332 stars in five trials, and 101 stars in one trial for the outer field.

TABLE 8

COMPLETENESS CORRECTIONS

	PERCENT COMPLETE		
V RANGE	Inner	Middle	Outer
14–15.....	100	100	...
15–16.....	100	100	...
16–17.....	100	100	100
17–18.....	100	100	100
18–19.....	100	100	100
19–20.....	83	100	100
20–21.....	83	100	100
21–22.....	63	100	100
22–23.....	30	84	100
23–24.....	8	84	76
24–25.....	...	82	...
25–26.....	...	34	...

The derived luminosity functions for the three fields are presented in Table 9. In this compilation, column (2) contains the number of field stars in the appropriate magnitude range, columns (3), (5), and (7) contain the number of stars actually counted on the CCD frames, while $N(V)$ for each field is the number in that magnitude range corrected for incompleteness and the background. These three luminosity functions are plotted together in Figure 13 after normalizing them so that they all have the same number of stars as the middle field in the magnitude interval $V = 20$–21. The luminosity function for the inner field is plotted with the thickest line, that for the outer field is indicated with the thinnest line, while the middle field luminosity function is plotted with a line of intermediate thickness. One sigma error bars are indicated at the bright and faint ends of these functions.

At the bright end of the luminosity function there is some

TABLE 9

LUMINOSITY FUNCTIONS IN THREE FIELDS OF M5

		INNER		MIDDLE		OUTER	
V RANGE (1)	BACKGROUND (2)	Number (3)	log $N(V)$ (4)	Number (5)	log $N(V)$ (6)	Number (7)	log $N(V)$ (8)
14–15.....	0	13	1.11	4	0.60	0	...
15–16.....	0	19	1.28	5	0.70	0	...
16–17.....	0	22	1.34	4	0.60	2	0.30
17–18.....	1	101	2.00	6	0.70	0	...
18–19.....	2	299	2.47	14	1.08	1	...
19–20.....	4	500	2.76	30	1.42	3	...
20–21.....	4	591	2.85	49	1.65	7	0.48
21–22.....	6	495	2.90	49	1.63	9	0.48
22–23.....	7	403	3.12	70	1.88	12	0.70
23–24.....	8	147	3.24	144	2.21	46	1.70
24–25.....	11	...	...	256	2.48	...	...
25–26.....	14	...	...	163	2.67	...	...

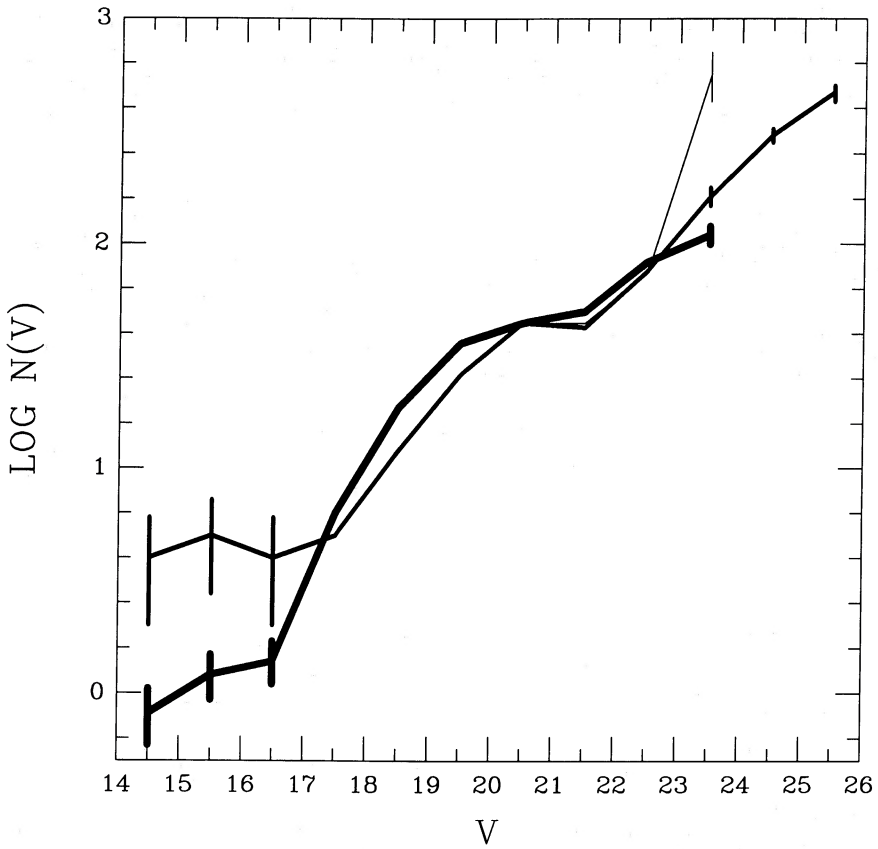

FIG. 13.—Luminosity functions for the three fields in M5 normalized so that they all have the same number of stars as the middle field in the magnitude range $V = 20$–21. The inner field luminosity function is plotted with the thickest line, while that for the outer field is shown with the thinnest line. One sigma error bars are given at the bright and faint ends of these functions.

evidence that there are more giants in the middle field than in the inner one. However, the numbers are very small, with only 13 stars actually counted in the middle field brighter than $V = 17.0$ Thus the difference in the two luminosity functions brighter than $V = 17$ is not very significant. In the magnitude interval $V = 17$–23 ($M_V = 2.7$–8.7), where the star-count statistics are good and the incompleteness corrections are small and well determined, all three functions are in good agreement. We conclude that in this magnitude range and over the three radii surveyed there is no obvious evidence that dynamical evolution in the cluster has had much effect in segregating stars of different mass at different distances from the center. In the middle field, where the stellar density is still appreciable but the crowding only modest, it was possible to trace the luminosity function to $V = 26$ ($M_V = 11.7$). No evidence of a turnover in the luminosity function is seen even though stars with masses as small as 0.3 $M_\odot$ are being observed.

At the faint end of the luminosity functions ($M_V = 9$–11) there is some evidence that mass segregation effects are, for the first time, being observed. The most distant field exhibits a large relative excess of faint objects over that of the middle field, while the inner one suggests a deficiency of faint stars. The effect appears to be real in so far as the differences observed are greater than those expected from the Poisson statistics of the counts themselves. Caution must be exercised, however, since the number of stars in the outer field is relatively small (only 80 stars in total counted of which 32 are expected to be unrelated to the cluster), while the completeness correction for the faintest bin in the inner field is large (each recovered star representing 12 stars actually present in the frame) and hence somewhat uncertain.

In order to formally quantify the mass segregation seen in Figure 13, we first determine the slope of the mass function [assumed to be a powerlaw of the form $\phi(m)dm = m^{-(1+x)}dm$] for each field. For this purpose we used theoretical luminosity functions calculated by VandenBerg (1986) using the models of VandenBerg and Bell (1985). Formal fits yielded a value of $x = 1.0$ for the inner field and $x = 1.5$ for the middle field. The uncertainty in these values is estimated to be ± 0.25 from a visual inspection of the fits. For the outer field, we estimate that the value of x exceeds 2.0.

At this point, it is worthwhile to note that observations similar to those discussed here (multiple-field luminosity functions) are the most natural and direct way of looking for mass segregation effects. There has been much theoretical work on this problem over the years (see, e.g., the review by Spitzer 1984) but, in examining the literature, we have been struck by the fact that the results are generally not presented in a manner which can be easily checked against the CCD observations which are now becoming available. Apart from this, there are at least two other factors which prevent a more detailed comparison with theory. (1) The studies in the literature generally do not involve realistic mass functions or incorporate more than a token range of masses for the member stars. (2) The velocity distribution of the cluster stars remains largely unknown and is an essential ingredient in the models. The most detailed published models appear to be for M3 (Gunn and Griffith 1979) and M2 (Pryor *et al.* 1986). Such

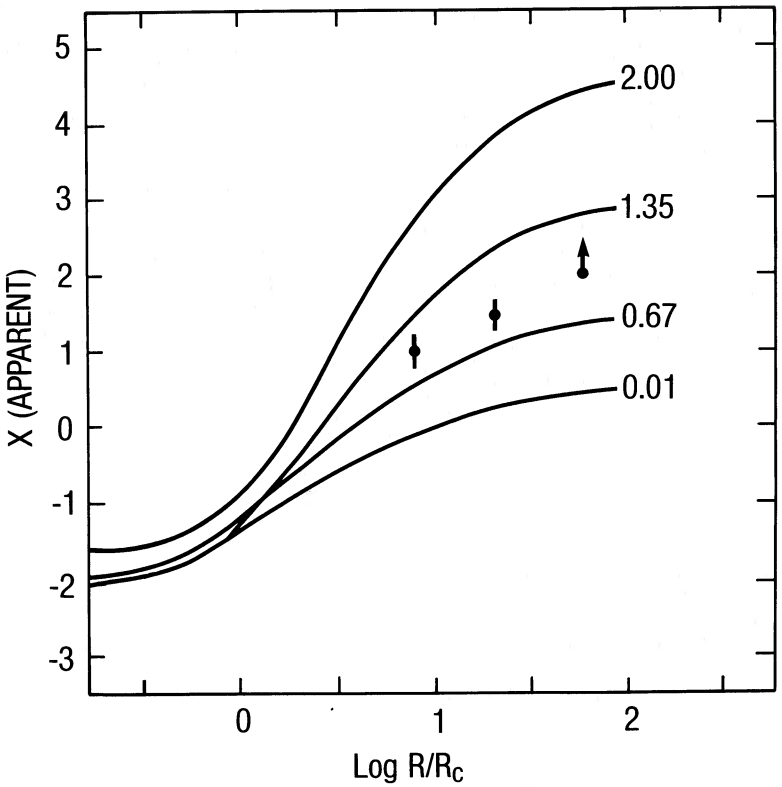

FIG. 14.—Plot of the apparent slope of the assumed power law mass function against radius (in units of the core radius) for multimass King models for a globular cluster with $c = 1.9$. Each model is labeled by the global value of the mass function. The three individual points plotted are the values of x found in the M5 fields observed at 8, 21, and 58 core radii. The observational data appear to follow these simple models rather well and imply that the global value of the mass function of M5 is near 1.0.

multicomponent quasi-thermal equilibrium models have mass segregation built in and can be used to calculate radial luminosity functions. Along these lines, Pryor, Smith, and McClure (1986) have recently constructed multimass King models with power-law mass functions in order to investigate the mass segregation corrections required for observed single-field globular cluster luminosity functions. In Figure 14 we plot their model appropriate for M5 [this is determined by the concentration of the cluster defined as $c = \log (R_t/R_c)$, where R_t and R_c are, respectively, the tidal and core radii of the cluster]. In this figure the ordinate is the value of x found in the local field observed at a distance of R/R_c core radii from the cluster center, while the model curves shown are labeled by the slope of the global mass function for the cluster. The three fields observed in M5 follow these simple models remarkably well—much better, in fact, than one would expect given some of the simplifications inherent in the calculations.

The deficiencies of these multimass King models as realistic representations of the mass segregation effects expected in globular clusters are fully discussed by Pryor, Smith, and McClure (1986). Nevertheless, it seems worthwhile to pursue these and similar calculations in view of the fact that observational constraints can now be provided by the deep ground-based CCD data.

VI. SUMMARY

We have secured deep *UBV* CCD data in three fields at different distances from the center of M5, and analysis has yielded the following results. (1) Color-magnitude diagrams constructed from these data show no radial effects and allow us to set an upper limit of 4% to any chemical abundance difference between a field at 8 core radii and one at 21. (2) The fundamental cluster parameters derived from our data are $E(B-V) = 0.02$, $[M/\mathrm{H}] = -1.13$, and $(m - M)_V = 14.30$. (3) From an overlay of the VandenBerg and Bell isochrones on to the cluster CMD, the best age estimate for M5 is 17 Gyr. (4) Radial luminosity functions give a hint that mass segregation is occurring for the faintest stars observed ($=0.3\ M_\odot$). However, for stars in the mass range $0.8\ M_\odot$ through $\sim 0.4\ M_\odot$, luminosity functions constructed in the three fields are identical within the errors and imply that the global slope of the power-law mass function in M5 is near 1.0.

The authors are indebted to CFHT for telescope time in support of their globular cluster program. This research is supported by grants from the Natural Sciences and Engineering Research Council of Canada.

REFERENCES

Arp, H. C. 1955, *A.J.*, **60**, 317.
———. 1962, *Ap. J.*, **135**, 31.
Bahcall, J. N. 1985, in *IAU Symposium 113, Dynamics of Star Clusters*, ed. J. Goodman and P. Hut (Dordrecht: Reidel), p. 481.
Bahcall, J. N., and Soneira, R. M. 1980, *Ap. J. Suppl.*, **44**, 73.
Buonanno, R., Corsi, C. E., and Fusi Pecci, F. 1981, *M.N.R.A.S.*, **196**, 435.
Burstein, D., Faber, S. M., and Gonzalez, J. J. 1986, *A.J.*, **91**, 1130.
Carney, B. W. 1979, *Ap. J.*, **233**, 211.
Christian, C. A., and Heasley, J. N. 1986, *Ap. J.*, **303**, 216.
Chun, M. S., and Freeman, K. C. 1979, *Ap. J.*, **227**, 93.

Davis, L. E. 1985, unpublished.
Fahlman, G. G., and Richer, H. B. 1987, in preparation.
Fahlman, G. G., Richer, H. B., and VandenBerg, D. A. 1985, *Ap. J. Suppl.*, **58**, 225.
Frogel, J. A., Cohen, J. G., and Persson, S. E. 1983, *Ap. J.*, **275**, 773.
Gunn, J. E., and Griffith, R. F. 1979, *A.J.*, **84**, 752.
Harris, W. E., and Hesser, J. E. 1985, in *IAU Symposium 113, Dynamics of Star Clusters*, ed. J. Goodman and P. Hut (Dordrecht: Reidel), p. 81.
Harris, W. E., and Racine, R. 1979, *Ann. Rev. Astr. Ap.*, **17**, 241.
King, I. R. 1962, *A.J.*, **67**, 471.
Landolt, A. U. 1983, *A.L.*, **88**, 439.
Lupton, R. H., and Gunn, J. E. 1986, *A.J.*, **91**, 317.
Lutz, T. E., and Kelker, D. H. 1973, *Pub. A.S.P.*, **85**, 573.
McClure, R. D., *et al.* 1986, *Ap. J. (Letters)*, **307**, L47.
McClure, R. D., Hesser, J. E., Stetson, P. B., and Stryker, L. L. 1985, *Pub. A.S.P.*, **97**, 665.
Osborn, W. H. 1971, PhD thesis, Yale University.
Penny, A. J., and Dickens, R. J. 1986, preprint.
Peterson, C. A. 1986, *Pub. A.S.P.*, **98**, 192.
Peterson, C. A., and King, I. R. 1975, *A.J.*, **80**, 427.
Pryor, C., McClure, R. D., Fletcher, J. M., Hartwick, F. D. A., and Kormendy, J. 1986, *A.J.*, **91**, 546.
Pryor, C., Smith, G. H., and McClure, R. D. 1986, *A.J.*, **92**, 1358.
Renzini, A. 1985, *Astronomy Express*, **1**, 4.
Richer, H. B., and Fahlman, G. G. 1984, *Ap. J.*, **277**, 227.
———. 1986, *Ap. J.*, **304**, 273.
Richer, H. B., and Fahlman, G. G. 1987, in preparation.
Sandage, A. 1969, *Ap. J.*, **158**, 1115.
———. 1970, *Ap. J.*, **162**, 841.
———. 1982, *Ap. J.*, **252**, 553.
Simoda, M., and Tanikawa, K. 1970, *Pub. Astr. Soc. Japan*, **22**, 143.
Smith, G. H., McClure, R. D., Stetson, P. B., and Hesser, J. E. 1986, *A.J.*, **91**, 842.
Spitzer, L., Jr. 1984, *Science*, **225**, 465.
Stetson, P. B. 1986, private communication.
VandenBerg, D. A. 1986, private communication.
VandenBerg, D. A., and Bell, R. A. 1985, *Ap. J. Suppl.*, **58**, 561.
Wallerstein, G. 1962, *Ap. J. Suppl.*, **6**, 407.
Wallerstein, G., and Carlson, M. 1960, *Ap. J.*, **132**, 276.
Webbink, R. F. 1985, in *IAU Symposium 113, Dynamics of Star Clusters*, ed. J. Goodman and P. Hut (Dordrecht: Reidel), p. 541.
Zinn, R. J. 1980, *Ap. J. Suppl.*, **42**, 19.
Zinn, R. J., and West, M. J. 1984, *Ap. J. Suppl.*, **55**, 5.

GREGORY G. FAHLMAN and HARVEY B. RICHER: Department of Geophysics and Astronomy, University of British Columbia, 2219 Main Mall, Vancouver, BC V6T 1W5, Canada